Electronic Supplementary Material (ESI) for Nanoscale.
This journal is © The Royal Society of Chemistry 2017

Electronic Supplementary Information (ESI)

MXene: A Potential Candidate for Yarn Supercapacitors

Jizhen Zhang[a], Shayan Seyedin[a,*], Zhoujie Gu[a], Wenrong Yang[b], Xungai Wang[a], and Joselito M. Razal[a,*]

[a] Deakin University, Institute for Frontier Materials, Geelong, VIC 3216, Australia.

[b] Deakin University, School of Life and Environmental Sciences, Geelong, VIC 3216, Australia

Email: joselito.razal@deakin.edu.au, shayan.seyedin@deakin.edu.au

Supplementary experimental

Materials

Ti_3AlC_2 powder (MAX phase) with particle size <40 μm was purchased from Carbon Ukraine and was used as supplied. Lithium fluoride (LiF, 98+%, Bio-Scientific) and hydrochloric acid (HCl, 37%, Sigma-Aldrich), phosphoric acid solution (H_3PO_4, 85 wt. % in water, Sigma-Aldrich), polyvinyl alcohol (PVA, M_w 89,000-98,000, Sigma-Aldrich) and poly(3,4-ethylenedioxythiophene)-poly(styrenesulfonate) (PEDOT-PSS) pellets (Orgacon™ Dry, Agfa) and carbon fiber (CF) yarns (Zoltek Panex 35) were used as received. Ethanol and acetone were purchased from Chem-Supply and were used as received. CF yarns were soaked in acetone, ethanol and water to remove the coating on their surface prior to being used as the substrate for fabricating the yarn supercapacitor (YSC) devices. The mass per length of CF yarns was measured as ~6.2 mg cm^{-1} and the diameter of a single filament CF was ~5 μm.

MXene synthesis

$Ti_3C_2T_x$ MXene (T_x denotes surface functional groups) was synthesized from the Ti_3AlC_2 MAX phase using the etching and exfoliation steps reported previously.[1] Briefly, LiF (~2.0 g) was first mixed with 30 mL of 6.0 M HCl in a 100 mL PTFE beaker. Ti_3AlC_2 powder (3.0 g) was then slowly added to the solution. The mixture was stirred at 40 °C for 45 hours to etch the Al layer. The suspension was diluted with deionized water and then centrifuged at 7,500 rpm for 15 minutes. This washing step was repeated several times until the pH of the supernatant reached ~7. The etched product containing the MXene flakes, was then collected *via* filtration using a 0.22 μm PTFE filter membrane. The collected MXene was then dried and stored under vacuum at room temperature before use.

Preparation of MXene/PEDOT-PSS coating formulations

The dry MXene powder (~200 mg) was dispersed in deionized (DI) water (10 mL) and the mixture was then sonicated with a water bath sonication for 1 hour to achieve the stock MXene suspension (20 mg mL^{-1}). PEDOT-PSS aqueous dispersion (4 mg mL^{-1}) was prepared separately by first dispersing the pellets (40 mg) in DI water (6 mL) and then the required amount of DI water was added to adjust the concentration. The MXene/PEDOT-PSS formulations were prepared by mixing the MXene suspension with the PEDOT-PSS suspension to achieve various ratios from 1:1 to 15:1. To avoid the oxidation of MXene, dispersions were purged with Argon during all processing steps that involved the use of MXene.

Fabrication of MXene-coated carbon fiber yarns

Yarn supercapacitors (YSCs) were fabricated by first preparing the MXene-based coated CF yarn electrodes. The electrodes were prepared by drop-casting a known amount of the formulation (*i.e.* pure MXene, pure PEDOT-PSS, and MXene/PEDOT-PSS composites) on loose CF yarns. The mass loading of the active materials was varied from 0.4 to 3.0 mg cm^{-1}. After the coating process, the samples were dried in a vacuum oven at room temperature for 12 hours. For high mass loadings of 2.0 and 3.0 mg cm^{-1}, the coating and vacuum drying processes were repeated several times until the desired loading was achieved.

Assembling of yarn supercapacitors

H_3PO_4/PVA gel electrolyte was separately prepared by dissolving PVA powder (6 g) in DI water (60 mL) at 85 °C with vigorous stirring and then adding H_3PO_4 (6 g) to the mixture following stirring until a homogeneous gel was achieved. MXene-based coated CF yarns were immersed in the gel electrolyte solution for ~5 min. Care was taken in this step to avoid contact of the CF substrate with the gel electrolyte solution. The samples were then placed in a vacuum

oven (room temperature) to remove any trapped bubbles and then the gel electrolyte layer was allowed to solidify at room temperature for ~6 hours. The YSC devices were prepared in three configurations as parallel, twisted, and face-to-face (Fig. S5). The parallel YSC device was achieved by closely placing two MXene-based coated CF yarn electrodes next to each other (length of each yarn ~3.5 cm), pre-coating with the gel electrolyte and then coating the 3 cm middle-section of the yarn electrodes again with the gel electrolyte. The thickness of the electrolyte was measured as ~30 μm and the mass of the electrolyte was in the range of 5.1 - 6.4 mg cm^{-1}. The YSCs in twisted configuration were prepared by inter-twisting two yarn electrodes (pre-coated with electrolyte) and then applying a thin electrolyte coating again. In order to achieve the YSC devices in face-to-face configuration, the MXene-based coated CF yarn electrodes (pre-coated with electrolyte) were first compressed to form ribbons (width and thickness ~2 mm and ~117.4 μm, respectively), placed on top of each other, and then coated again with a thin layer of the electrolyte. The steps used in the preparation of the YSC in face-to-face configuration is schematically shown in Fig. 1A (main text). The YSC devices were dried under vacuum at room temperature for 12 hours before testing.

Characterization

X-ray diffraction (XRD) analyses were carried out using a powder diffractometer (PANalytical X'Pert Powder) using Cu Kα radiation (λ = 1.54 Å) at a 2θ scan step of 0.013° and 100 s dwell time. A scanning electron microscope (SEM, Zeiss Supra 55VP, Germany) was used to study the morphology of the samples.

The electrochemical properties of the YSCs were studied using cyclic voltammetry (CV), galvanostatic charge-discharge (GCD), and electrochemical impedance spectroscopy (EIS) with an electrochemical workstation (BioLogic SP-300). CVs and GCDs were recorded at a potential window of 0 to 0.5 V at the scan rates ranging from 2 to 200 mV s^{-1} and at the specific

current per length of 0.2 to 4.0 mA cm^{-1}, respectively. EIS measurements were performed at open circuit potential by applying an alternating-current voltage with 10 mV amplitude in a frequency range of 10 mHz to 200 kHz. YSC devices were pre-cycled using CV at 100 mV s^{-1} for 20 cycles prior to recording the electrochemical data. A timer with a power of ~3.1 μW (nominal voltage 1.5 V) was used for the demonstration purpose.

The capacitance of YSC device (C_D) was calculated from the CV and GCD curves according to the Eqs. S1 and S2 respectively.

$$C_D = \frac{\int I dU}{2v\Delta U} \quad \text{(S1)}$$

$$C_D = \frac{I}{(dU/dt)} \quad \text{(S2)}$$

where I in Eqs. S1 and S2 is the current and the discharge current respectively, v is the potential scan rate (V s^{-1}), ΔU is the potential window (V), and dU/dt is the slope of the discharge curve in GCD.

The values of length capacitance (C_L, mF cm^{-1}), gravimetric capacitance (C_M, F g^{-1}), areal capacitance (C_S, mF cm^{-2}) and volumetric capacitance (C_V, F cm^{-3}) of the YSC devices were calculated based on the device capacitance (C_D) using Eqs. S3, S4, S5 and S6 respectively.

$$C_L = \frac{C_D}{L} \quad \text{(S3)}$$

$$C_M = \frac{2C_D}{m} \quad \text{(S4)}$$

$$C_S = \frac{C_D}{S} \quad \text{(S5)}$$

$$C_V = \frac{C_D}{V} \quad \text{(S6)}$$

where l denotes the length of the YSC device, m is the mass of a single electrode, and S and V are the surface area and volume of the whole device (including the electrolyte), respectively.

For a symmetric SC with two identical electrodes, we have $C_{electrode} = 2C_D$. The length capacitance (C_l, mF cm^{-1}) and gravimetric capacitance (C_m, F g^{-1}) of single electrode were calculated from Eqs. S7 and S8 respectively.

$$C_l = \frac{2C_D}{l} \quad \text{(S7)}$$

$$C_m = \frac{4C_D}{m} \quad \text{(S8)}$$

In these equations l and m denote the length and the mass of a single electrode, respectively.

The capacitance retention (C_r) was calculated from the specific capacitance of the YSC device (C_i) in the cycle i and the specific capacitance in the first cycle (C_1) using the equation S9.

$$C_r = \frac{C_i}{C_1} \times 100\% \quad \text{(S9)}$$

The relationship between resistance (R) and electrode dimensions is explained by the following equation:

$$R = \frac{\rho l}{A} \quad \text{(S10)}$$

where ρ is the specific resistance, l is the length and A is the cross-sectional area of the electrode.

Identifying the YSC device configuration

YSCs have been fabricated in three device configurations: parallel, twisted, and face-to-face (Fig. S5A). When we used the parallel or twisted configurations, crease appeared when the

device was bent (Fig. 5B and C). In contrast, the formation of crease was not observed on the device with face-to-face configuration suggesting better flexibility than the other two configurations. To investigate the influence of device configurations on performance, we compared the performance of YSCs made from 6 cm electrodes assembled in parallel, twisted, and face-to-face configurations. As shown in Fig. S6A, all devices showed similar performance when the scan rate is 2 mV s^{-1} (length capacitance ~0.22 mF cm^{-1}). However, the face-to-face configuration showed the best performance when the scan rate is 1,000 mV s^{-1} (Fig. S6B). The analysis of the length capacitance of the YSC devices made from pure CF (Fig. S6C) showed that when the scan rate reached 1,000 mV s^{-1}, the length specific capacitance of the device in the face-to-face configuration (~0.06 mF cm^{-1}) was almost two times higher than the YSC devices in twisted (~0.04 mF cm^{-1}) and parallel (~0.03 mF cm^{-1}) configurations.

Carbon fiber yarns with the same cross-sectional area were used as electrodes in the three configurations. Hence, we estimate (Eq. S10) that all electrodes have the same resistance. This result was also confirmed when the EIS curve was normalized by the length of electrode, as shown in the Nyquist plots (Fig. S6D).

The face-to-face configuration can achieve smaller electrode distance compared with the parallel and twisted configurations (Fig. S7), resulting in a more effective ion diffusion. As shown in Fig. S5E, the -45° phase angle, *i.e.* the point at which the resistive and capacitive impedances are equal, was present at 47 Hz for face-to-face, at 16 Hz for twisted and at 11 Hz for parallel, demonstrating the fast accessibility of the ions in face-to-face configurations.[2] Because of the superiority of the face-to-face configuration compared to the other two approaches, we fabricated the MXene-based coated CF YSC devices using this configuration.

Supplementary results

Table S1 Comparison of the electrochemical performance of MXene-based coated CF YSC with relevant literature reports.

Structure	Electrode material	Electrolyte	Length (cm)	C_L (mF cm^{-1})	C_M (F g^{-1})	C_S (mF cm^{-2})	C_V (F cm^{-3})	Ref.
Face-to-face	MXene/PEDOT-PSS coated CF	PVA[5]/H_3PO_4	3	131.7	16.1	658.5	54.7	This work
Coaxial	CNTs[1]/CF bundles/CNT film	PVA/H_3PO_4	5	6.3	80	86.8	~50	3
	Coaxial graphene fiber	PVA/H_2SO_4		4.63	185	204	--	4
Textiles	KOH treated CF	PVA/H_3PO_4	--	--	197	500	--	5
	Activated carbon coated cellulose yarns	PVA/ Silicotungstic acid/ H_3PO_4	--	37	--	--	--	6
	Activated carbon coated CF cloth	PVA/ Silicotungstic acid/ H_3PO_4	--	--	63-88	190-660	--	7
Parallel	MnO_2/CF core-shell structure	PVA/H_3PO_4	--	--		--	2.5	8
	MXene coated silver-plated nylon fibers	PVA/H_2SO_4	5	50	--	328	--	9
	PPy[2]/MnO_2/CNT/ cotton thread	PVA/H_3PO_4	--	--	--	1490	--	10
	PEDOT-PSS/CNT biscrolled yarn	PVA/H_2SO_4	7.5	0.46	--	73	179	11
Twisted	Activated carbon/CF	PVA/H_3PO_4	10	45.2	82.1	--	--	12
	PPy/MnO_2/graphene modified steel yarn	PVA/H_3PO_4	--	31	--	411	68.5	13
	PANI[3]/functionalized CF	PVA/H_3PO_4	10	3.9				14
	Oxidized CF	PVA/H_3PO_4	--	--	--	--	14.2	15
	Niobium nanowires/PEDOT yarn	PVA/H_2SO_4	6	--	12	52	50	16
	Graphene/CNT fiber	PVA/H_3PO_4	--	5.3	--	177	158	17
	RGO[4]/Ni cotton yarn	PVA/LiCl	10	~110	311	--	--	18

[1] Carbon nanotubes, [2] Polypyrrole, [3] Polyaniline, [4] Reduced graphene oxide, [5]Polyvinyl alcohol

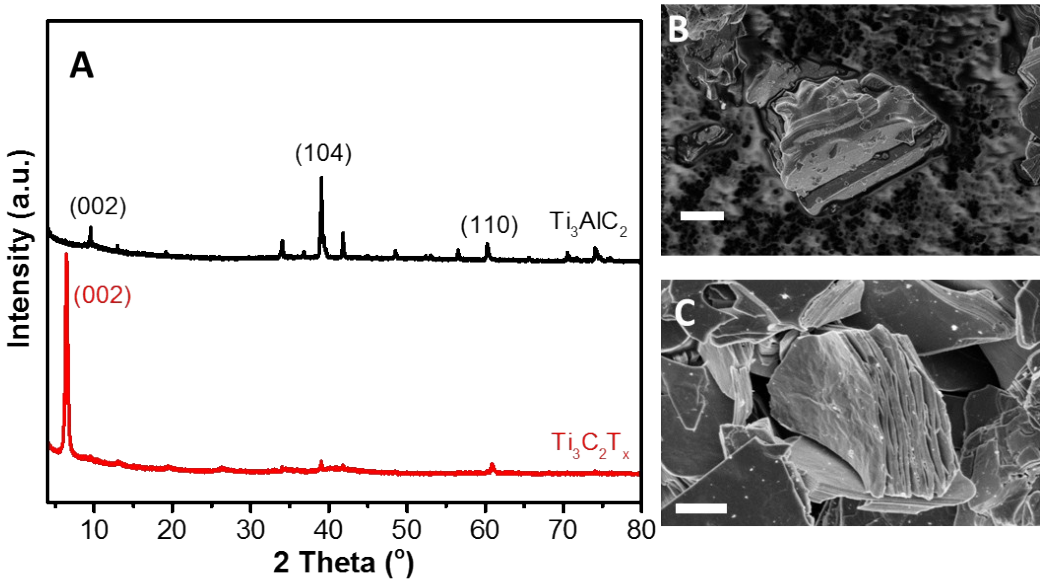

Fig. S1 (A) XRD spectra of MAX phase and MXene. SEM images of (B) MAX phase and (C) MXene. Scale bars in SEM images are 1 μm.

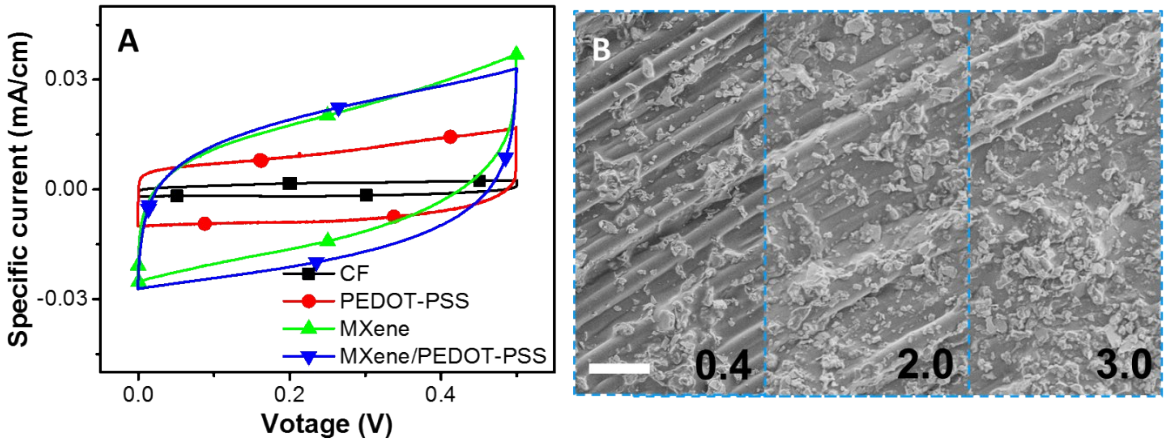

Fig. S2 (A) CV curves of YSCs with different coating formulations. All samples have a total mass loading of 0.4 mg cm^{-1} and all CVs were obtained 2 mV s^{-1}. (B) SEM images of CF yarns coated with MXene/PEDOT-PSS formulations at different loadings of 0.4, 2.0, and 3.0 mg cm^{-1}. The scale bar is 10 μm for all images.

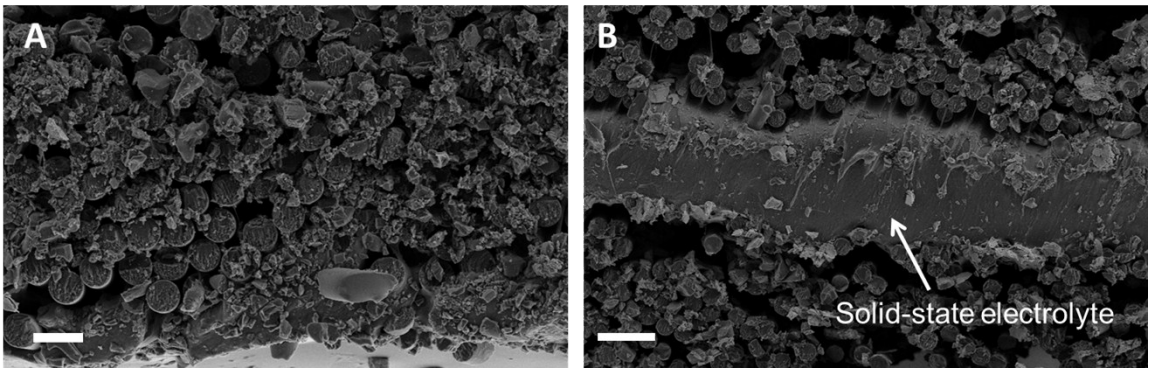

Fig. S3 Cross-section SEM images of (A) electrode and (B) YSC obtained from CF coated with MXene formulation (2.0 mg cm-1). The scale bars in A and B are 10 μm and 20 μm, respectively.

Table S2 Comparison of the changes in properties of carbon fiber electrode before and after coating with MXene/PEDOT-PSS formulation (9:1 ratio, mass loading 2.0 mg cm-1).

	Mass ($mg\ cm^{-1}$)	Thickness (μm)	Resistance of 1 cm long CF yarn (Ω)	Conductivity ($S\ cm^{-1}$)	Tensile strength (GPa)	Strain (%)
Before coating	~6.2	~117.4	~2.2	~194	~3.1	~1.6
After coating	~8.2	~120.3	~2.1	~198	~3.0	~1.6

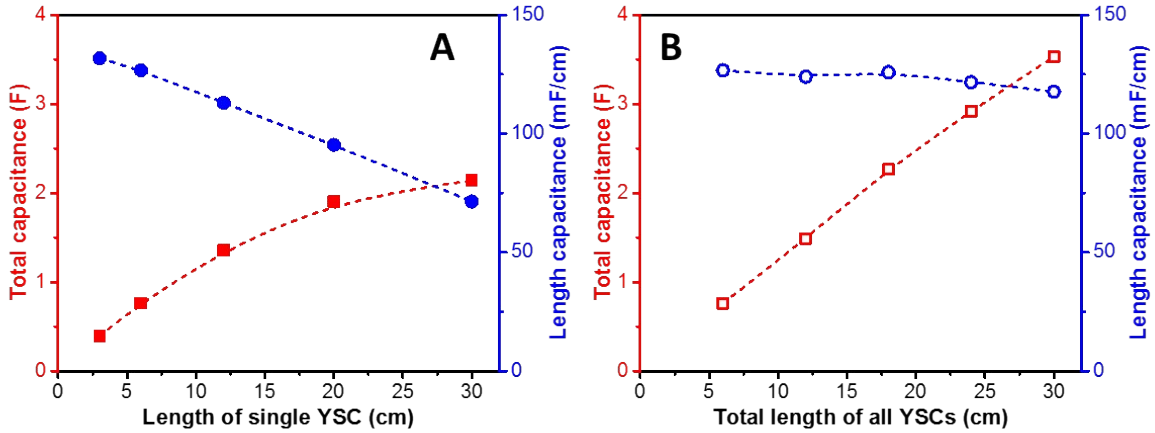

Fig. S4 The total capacitance and length specific capacitance of YSCs when (A) the electrode length increases in a single YSC device and (B) when each 6 cm YSC is electrically connected in parallel. The total length in B is the sum of the YSC length depending on the number of the parallel connections.

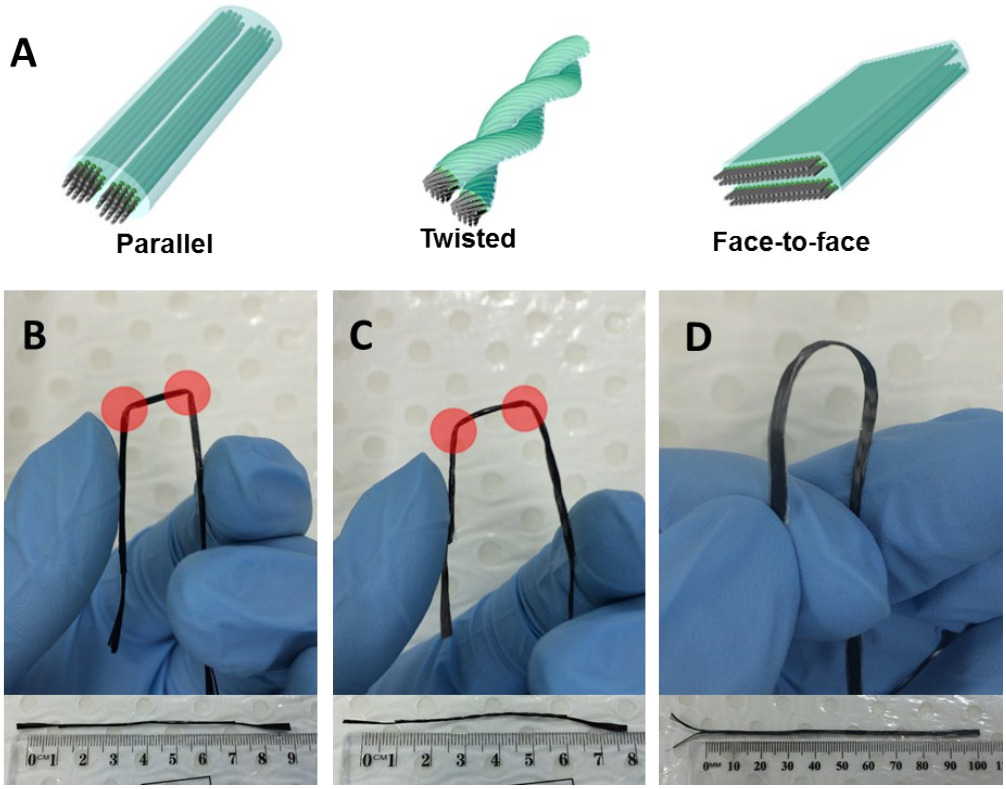

Fig. S5 (A) Schematic representation of the three YSC device configurations. (B-D) Digital photographs of the different YSC devices when bent 180°. The photographs of the original devices correspond to the device configurations at the top of each image.

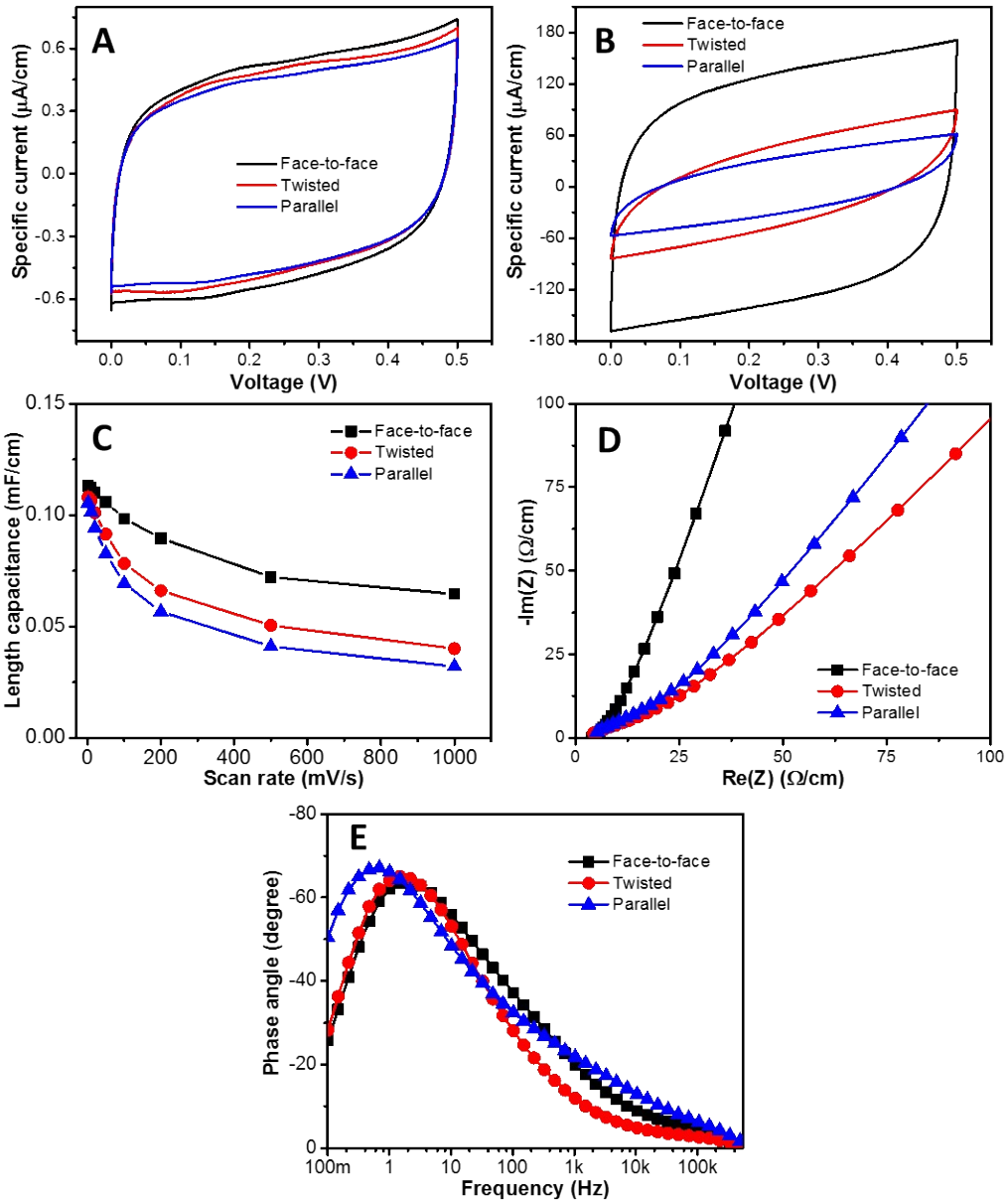

Fig. S6 CV curves at (A) 2 mV s^{-1} and (B) 1 V s^{-1}, (C) length capacitance versus scan rate, (D) Nyquist plots and (E) Impedance phase angle as a function of frequency of the CF-based YSC devices prepared using three different configurations.

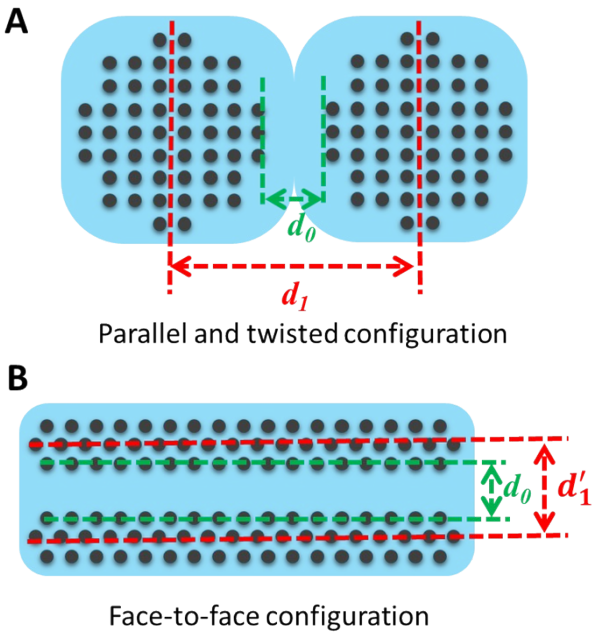

Fig. S7 Cross-sections of device configurations in (A) parallel and twisted configurations and (B) face-to-face configuration.

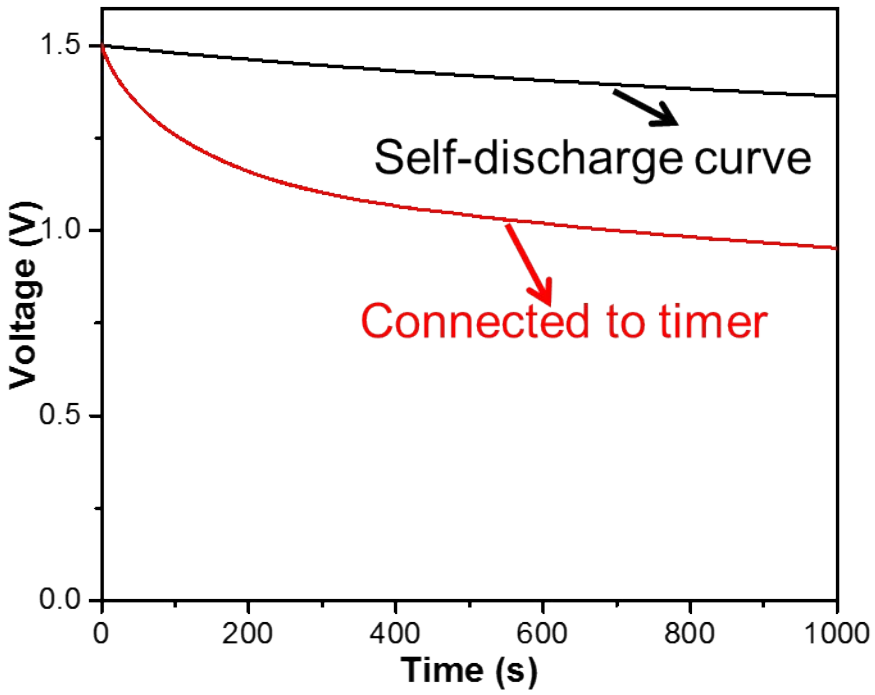

Fig. S8 Comparison of the open circuit potential for three YSCs connected in series during self-discharge and when connected to a timer with a power of ~3.1 μW.

References

1. M. Ghidiu, M. R. Lukatskaya, M. Q. Zhao, Y. Gogotsi and M. W. Barsoum, *Nature*, 2014, **516**, 78-81.
2. Z. S. Wu, K. Parvez, X. Feng and K. Müllen, 2013, **4**, 2487.
3. V. T. Le, H. Kim, A. Ghosh, J. Kim, J. Chang, Q. A. Vu, D. T. Pham, J.-H. Lee, S.-W. Kim and Y. H. Lee, *ACS nano*, 2013, **7**, 5940-5947.
4. X. Zhao, B. Zheng, T. Huang and C. Gao, *Nanoscale*, 2015, **7**, 9399-9404.
5. T. Zhang, C. H. J. Kim, Y. Cheng, Y. Ma, H. Zhang and J. Liu, *Nanoscale*, 2015, **7**, 3285-3291.
6. K. Jost, D. P. Durkin, L. M. Haverhals, E. K. Brown, M. Langenstein, H. C. De Long, P. C. Trulove, Y. Gogotsi and G. Dion, *Adv. Energy Mater.*, 2015, **5**, 1401286.
7. K. Jost, D. Stenger, C. R. Perez, J. K. McDonough, K. Lian, Y. Gogotsi and G. Dion, *Energ. Environ. Sci.*, 2013, **6**, 2698-2705.
8. X. Xiao, T. Li, P. Yang, Y. Gao, H. Jin, W. Ni, W. Zhan, X. Zhang, Y. Cao, J. Zhong, L. Gong, W.-C. Yen, W. Mai, J. Chen, K. Huo, Y.-L. Chueh, Z. L. Wang and J. Zhou, *ACS nano*, 2012, **6**, 9200-9206.
9. M. Hu, Z. Li, G. Li, T. Hu, C. Zhang and X. Wang, *Adv.Mater. Technol.*, 2017, **2**, 1700143.
10. N. Liu, W. Ma, J. Tao, X. Zhang, J. Su, L. Li, C. Yang, Y. Gao, D. Golberg and Y. Bando, *Adv. Mater.*, 2013, **25**, 4925-4931.
11. J. A. Lee, M. K. Shin, S. H. Kim, H. U. Cho, G. M. Spinks, G. G. Wallace, M. D. Lima, X. Lepró, M. E. Kozlov, R. H. Baughman and S. J. Kim, *Nat. Commun.*, 2013, **4**, 1970.
12. S. Zhai, W. Jiang, L. Wei, H. E. Karahan, Y. Yuan, A. K. Ng and Y. Chen, *Mater. Horiz.*, 2015, **2**, 598-605.
13. Y. Huang, H. Hu, Y. Huang, M. Zhu, W. Meng, C. Liu, Z. Pei, C. Hao, Z. Wang and C. Zhi, *ACS nano*, 2015, **9**, 4766-4775.
14. H. Jin, L. Zhou, C. L. Mak, H. Huang, W. M. Tang and H. L. W. Chan, *Nano Energy*, 2015, **11**, 662-670.
15. D. Yu, S. Zhai, W. Jiang, K. Goh, L. Wei, X. Chen, R. Jiang and Y. Chen, *Adv. Mater.*, 2015, **27**, 4895-4901.
16. S. M. Mirvakili, M. N. Mirvakili, P. Englezos, J. D. W. Madden and I. W. Hunter, *ACS Appl. Mater. Interfaces*, 2015, **7**, 13882-13888.
17. L. Kou, T. Huang, B. Zheng, Y. Han, X. Zhao, K. Gopalsamy, H. Sun and C. Gao, *Nat. Commun.*, 2014, **5**, 3754.
18. L. Liu, Y. Yu, C. Yan, K. Li and Z. Zheng, *Nat. Commun.*, 2015, **6**, 7260.